

How to Cite:

Muthuboopathi, G., & Shanmugarajan, T. S. (2022). Synthesis, characterization, In-Silico studies, and anti-inflammatory activity of Novel Imidazole-5(4H)-Ones. *International Journal of Health Sciences*, 6(S1), 6816–6834. <https://doi.org/10.53730/ijhs.v6nS1.6445>

Synthesis, characterization, *In-Silico* studies, and anti-inflammatory activity of Novel Imidazole-5(4H)-Ones

G. Muthuboopathi

Department of Pharmaceutics, School of Pharmaceutical Sciences, Vels Institute of Science, Technology & Advanced Studies (VISTAS), Chennai, 600117, Tamil Nadu, India.

T.S.Shanmugarajan

Department of Pharmaceutics, School of Pharmaceutical Sciences, Vels Institute of Science, Technology & Advanced Studies (VISTAS), Chennai, 600117, Tamil Nadu, India.

Corresponding author email: mailshanmuga@gmail.com

Abstract---Several new imidazole-5(4H)-one analog was synthesized using multi-step synthesis. All the synthesized compounds were characterized using FT-IR, ¹H-NMR, Mass spectroscopy, and microanalysis to confirm their chemical structure. Molecular properties of the title compounds were predicted using Molinspiration online tool and binding studies of the title analogs against COX-1 & COX-2 were predicted by the molecular docking method. All novel imidazole-5(4H)-one analog were tested for their *in-vivo* anti-inflammatory activity using carrageenan-induced paw edema test in *Wistar* rats. Varying degree (weak to excellent) of anti-inflammatory activity was displayed by title compounds. In addition, *in vitro* anticancer potency of test compounds was estimated by the MTT assay method and found that most of the tested analogs were found to be inactive at 10 μM concentration against the tested cell lines. Among twelve tested title compounds, 2-methyl-1-(4-methyl piperazine-1-yl)-4-(naphthalen-1-ylmethylene)-1H-imidazol-5(4H)-one AL01, and 4-benzylidene-2-methyl-1-(4-methylpiperazin-1-yl)-1H-imidazol-5(4H)-one AL02 displayed more potent anti-inflammatory activity which is slightly higher than reference diclofenac.

Keywords---Imidazole, Benzylidene, Furan, In-silico studies, Molecular docking, Anti-inflammatory.

Introduction

Inflammation is part of the body's defense mechanism and plays a role in the healing process. When the body detects an intruder, it launches a biological response to try to remove it. The attacker could be a foreign body, such as a thorn, an irritant, or a pathogen. Pathogens include bacteria, viruses, and other organisms, which cause infections. Sometimes, the body mistakenly perceives its cells or tissues as harmful. This reaction can lead to autoimmune diseases, such as type 1 diabetes. Experts believe inflammation may contribute to a wide range of chronic diseases. Universally NSAIDs (Nonsteroidal anti-inflammatory drugs) are one of the most important common healing groups of drugs employed for the management of fever, pain, and inflammation.¹ In contrast, the efficiency of NSAIDs was narrowed due to increased occurrence of the sensible GI (gastrointestinal) damage primarily ulceration of GI and its connected perforation and complications.²

Heterocyclic compounds are those cyclic compounds whose rings contain besides, carbon, one or more atoms of other elements. Heterocyclic compounds are very widely distributed in nature and are particularly important because of the wide variety of physiological activities associated with this class of substances. All the heterocyclic compounds have a great interest in pharmaceutical chemistry. Out of these heterocyclic compounds, imidazole and its derivatives have a wide variety of biological activities.³⁻⁸ Imidazole is an important group of heterocyclic compounds that are biologically active and of significant importance in medicinal chemistry. The imidazole ring is an important pharmacophore in modern drug discovery.

Imidazole has emerged as an anti-inflammatory agent because of its broad spectrum of *in-vitro* and *in-vivo* chemotherapeutic activities.⁹⁻¹³ the biological activities exhibited by compounds containing imidazole moiety have prompted chemists to synthesis more and more imidazole libraries and screen them for potential activities. Based on these findings, we decided to synthesize some novel imidazole-5(4*H*)-one derivative by multi-step synthesis and evaluated its *in-vivo* anti-inflammatory activity with the hope to obtain more active anti-inflammatory agents. In addition, title compounds were also tested *in-silico* for predicting ADME, molecular properties, and toxicity of title compounds.

Experimental Materials & Methods

The chemicals and reagents used were obtained from various chemical units Qualigens, E. Merck India Ltd., CDH, and SD Fine Chem. These solvents used were of LR grade and purified before their use. The silica gel G used for analytical chromatography (TLC) was obtained from E. Merck India Ltd. All the melting points were taken in an open glass capillary and are uncorrected. ¹H-NMR spectra were recorded at 400 MHz on Bruker Avance-400 NMR spectrometer in CDCl₃ using tetramethylsilane (TMS) as an internal standard. ¹³C-NMR spectra were recorded at 101 MHz in CDCl₃. The chemical shifts are reported on a ppm scale. Mass spectra were obtained on a JEOL-SX-102 instrument using electron impact

ionization. All the IR spectra were recorded in KBr pellets on a Jasco FT-IR 410 spectrometer.

Software Required

From www.scripps.edu, AutoDock 4.2, and MGL (molecular graphics laboratory) tools were downloaded. Chemdraw ultra for sketching and chem 3D Pro for energy minimization and convert chem draw file into PDB format. Install Molegro Molecular viewer from (<http://molexus.io/molegro-molecular-viewer>) from which protein can be preprocessed, binding pocket interactions can be accessed, the docked complex can be explored.

Predictions of Physicochemical Properties and ADMET

In the drug discovery process, physicochemical properties by 5-Lipinski's rule were observed for predicting the bioactive drug in the oral route.¹⁴ In pharmacokinetic studies, screening of ADME properties is evaluated for understanding their bioavailability.¹⁵ Additionally, molecular properties and toxicity were evaluated by the online tool in the organic portal web of preADMET and molinspirations.¹⁶

Molecular Docking

Computer-aided drug design is one of the tools which plays a vital role in understanding the structure-activity relationship, binding energy, the interaction between the protein and ligand, binding affinity, etc. In this program, Auto dock was widely used in evaluating the binding studies of our ligand (synthesized compound **AL01-AL12**) with our target enzymes. This program helps us to predict how these small molecules of synthesized derivatives may bind with the targeted enzyme COX-1 (ID of PDB: 3KK6) & COX-2 (ID of PDB: 3LN1). <http://www.rcsb.org/pdb> (RCSB Protein Data Bank (PDB) database) was used to retrieve the targeted enzyme.

Preparation of Protein

Before starting the molecular docking, the water molecules were removed from the respective proteins. The selected enzymes from the protein data bank were subjected to Molegro viewer by which those enzymes were refined.

Preparation of Ligand

The structures of ligands were drawn using Chem Draw software. The protein file (PDB) was being further optimized by adding hydrogen atoms and removing water molecules. The end up with all these procedures, the protein and ligand were well prepared for docking.

Grid Box Preparation and Docking

Chem draw ultra was used to convert all files needed for the docking study. Parameters of the Grid box were fixed in such a way to permit for an appropriately-sized cavity space large sufficient to accommodate every analog

within the binding site of each protein and were estimated using AutoDock Tools. Into the corresponding protein structures, entire co-crystallized inhibitory ligands are re-docked to allow comparison between docking scores and validate the accuracy. Based on their energy scores ligands are ranked and searched at different orientations of ligands. Concerning its biological confirmation for each control ligand, a similar docking pose was obtained in the co-crystallized protein-ligand complex using our docking protocol. For each ligand best conformational space was explored with a 150 individual population size during the process of docking using the Lamarckian Genetic Algorithm. The rest of the parameters were fixed default. Some control inhibitors and the active binding sites of selected enzymes are well documented.¹⁷⁻²⁰ Docking efficiency was increased using a guided docking approach.²¹ In this approach, in each protein binding site, each ligand conformation (including re-docking of the control inhibitors) was measured. Later, to forecast the top protein-ligand binding affinities scoring function was used to rank these conformations (Table 4 & Table 5). Highest predicted ligand/protein affinity was indicated by the lowest binding free energy. Biovia Discovery studio visualizer was used to visualize the specific intermolecular interactions with the targets (Figure 1 & Figure 2).

General procedure

Synthesis of 2,4-disubstituted oxazol-5(4*H*)-one (III-VI)

A mixture of N-substituted glycine **I-II** (0.01 mol), aromatic aldehyde (0.01 mol), fused sodium acetate (0.82 g; 0.01 mol), and acetic anhydride (3.06 g; 0.03 mol) was refluxed in a boiling water bath for 3 h. Ethanol (95 %; 10 ml) was added to the flask after cooling and the mixture was left aside at 5°C for 4–6 h. The precipitate formed was filtered and washed with cold ethanol, then with boiling water, and again with cold ethanol. The dried precipitate was recrystallized using acetic acid.

2-Methyl-4-(naphthalen-1-ylmethylene) oxazol-5(4*H*)-one (III): Yield = 75 %, m.p. 193-194 °C. IR (KBr cm^{-1}) ν max: 3012, 2955, 1709, 1641, 1617, 1530, 1315, 1283, 760. ¹H NMR (400 MHz, CDCl_3) δ 8.39 (d, J = 7.0 Hz, 1H), 8.02 – 7.54 (m, 3H), 7.42 – 7.08 (m, 3H), 7.01 (s, 1H), 2.51 (s, 3H). ¹³C NMR (101 MHz, CDCl_3) δ 170.14, 153.78, 138.27, 132.82, 131.64, 131.02, 130.70, 130.19, 129.53, 128.40, 128.18, 126.06, 125.79, 124.13, 119.58, 22.96. ESIMS m/z : 238.40 [$M + H$]⁺ calcd for $\text{C}_{15}\text{H}_{11}\text{NO}_2 + \text{H}^+$ (237.54).

4-Benzylidene-2-methyloxazol-5(4*H*)-one (IV): Yield = 83 %, m.p. 156-159 °C. IR (KBr cm^{-1}) ν max: 3037, 2960, 1715, 1643, 1608, 1546 1332, 1289, 765. ¹H NMR (400 MHz, CDCl_3) δ 8.35 – 8.19 (m, 2H), 7.72 – 7.50 (m, 3H), 7.26 (s, 1H), 2.63 (s, 3H). ¹³C NMR (101 MHz, CDCl_3) δ 163.19, 155.03, 138.86, 135.59, 130.12, 129.31, 124.28, 118.71, 26.05. ESIMS m/z : 206.48 [$M + \text{H}_2\text{O}$]⁺ calcd for $\text{C}_{11}\text{H}_9\text{NO}_2 + \text{H}_2\text{O}^+$ (205.27).

2-(Furan-2-yl)-4-(naphthalen-1-ylmethylene)oxazol-5(4*H*)-one (V): Yield = 87 %, m.p. 171-172 °C. IR (KBr cm^{-1}) ν max: 3023, 2946, 1708, 1626, 1530, 1342, 1288, 764. ¹H NMR (400 MHz, CDCl_3) δ 8.24 – 7.90 (m, 3H), 7.53 – 7.39 (m, 2H), 7.25 – 7.03 (m, 2H), 6.98 (s, 1H), 6.73 (d, J = 4.0 Hz, 1H), 6.67 (d, J = 2.5 Hz, 1H), 6.62 (d, J = 2.8 Hz, 1H). ¹³C NMR (101 MHz, CDCl_3) δ 168.19, 165.70, 145.95, 144.08,

135.92, 134.64, 132.50, 131.72, 128.19, 127.82, 125.43, 124.17, 123.98, 123.54, 120.78, 116.11, 112.56, 111.03. ESIMS m/z : 308.48[M + H₂O]⁺ calcd for C₁₈H₁₁NO₃ + H₂O (307.24).

4-Benzylidene-2-(furan-2-yl)oxazol-5(4H)-one (VI): Yield = 76 %, m.p. 167-169 °C. IR (KBr cm⁻¹) ν max: 3046, 2961, 1712, 1650, 1628, 1546, 1523, 1478, 1359, 1280, 1176, 761. ¹H NMR (400 MHz, CDCl₃) δ 7.59 (d, J = 1.8 Hz, 1H), 7.42 – 7.26 (m, 2H), 7.18 – 7.03 (m, 2H), 6.97 (s, 1H), 6.91 (d, J = 3.5 Hz, 1H), 6.85 (d, J = 3.0 Hz, 1H), 6.68 (d, J = 7.9 Hz, 1H). ¹³C NMR (101 MHz, CDCl₃) δ 170.12, 163.56, 147.79, 145.23, 134.95, 130.38, 129.06, 128.72, 125.47, 117.65, 110.91, 108.28. ESIMS m/z : 258.39 [M + H₂O]⁺ calcd for C₁₄H₉NO₃ + H₂O⁺ (257.46).

Synthesis of 1,2,4-trisubstituted-1H-imidazol-5(4H)-one (AL01-AL12)

A mixture of 2,4-disubstituted oxazol-5(4H)-one **III-VI** (0.01 mol) and various aromatic amines (0.01 mol) in glacial acetic acid (25 ml) was refluxed in a boiling water bath for 15 h. After the completion of the reaction (TLC-monitoring), the reaction mixture was allowed to cool down to room temperature and poured into ice-cold water with constant stirring. The solid separated was filtered, washed with water, dried, and crystallized using ethanol.

2-Methyl-3-(4-methylpiperazin-1-yl)-5-(naphthalen-1-ylmethylene)-3,5-dihydro-4H-imidazol-4-one (AL01): Yield = 79 %, m.p. 240-242 °C. IR (KBr cm⁻¹) ν max: 3049, 2960, 1713, 1646, 1604, 1531, 1345, 1277, 762. ¹H NMR (400 MHz, CDCl₃) δ 8.75 (d, J = 7.3 Hz, 1H), 8.27 (d, J = 8.4 Hz, 1H), 7.95 – 7.83 (m, 3H), 7.66 – 7.39 (m, 3H), 4.01 (s, 2H), 2.89 (s, 4H), 2.36 (s, 3H), 2.35 (s, 3H), 2.27 (s, 2H). ¹³C NMR (101 MHz, CDCl₃) δ 169.48, 164.42, 137.60, 133.66, 132.56, 131.29, 130.70, 129.87, 129.17, 129.09, 128.91, 127.11, 126.93, 126.50, 126.40, 126.00, 125.76, 125.50, 123.28, 123.06, 122.41, 55.26, 51.55, 45.87, 15.02. ESIMS m/z : 335.30 [M + H]⁺ calcd for C₂₀H₂₂N₄O + H⁺ (334.42).

5-Benzylidene-2-methyl-3-(4-methylpiperazin-1-yl)-3,5-dihydro-4H-imidazol-4-one 9AL02): Yield = 76 %, m.p. 222-224 °C. IR (KBr cm⁻¹) ν max: 3015, 2949, 1702, 1632, 1616, 1530, 1349, 1297, 773. ¹H NMR (400 MHz, CDCl₃) δ 8.13 – 8.05 (m, 2H), 7.45 – 7.31 (m, 3H), 7.01 (s, 1H), 3.97 (s, 2H), 2.85 (d, J = 10.4 Hz, 4H), 2.33 (d, J = 1.9 Hz, 6H), 2.26 (d, J = 11.2 Hz, 2H). ¹³C NMR (101 MHz, CDCl₃) δ 169.54, 163.75, 136.88, 134.08, 132.15, 130.12, 128.72, 127.25, 77.35, 77.04, 76.72, 55.22, 51.47, 45.83, 14.97, 0.01. ESIMS m/z : 285.30 [M + H]⁺ calcd for C₁₆H₂₀N₄O + H⁺ (284.36).

3-(1-Benzylpiperidin-4-yl)-2-(furan-2-yl)-5-(naphthalen-1-ylmethylene)-3,5-dihydro-4H-imidazol-4-one (AL03): Yield = 80 %, m.p. 238-239 °C. IR (KBr cm⁻¹) ν max: 3469, 3414, 3236, 2932, 1652, 1619, 1544, 1351, 1295, 775. ¹H NMR (400 MHz, CDCl₃) δ 7.92 – 7.81 (m, 3H), 7.56 – 7.49 (m, 2H), 7.48 – 7.41 (m, 2H), 7.38 (s, 1H), 7.32 (dt, J = 6.4, 1.4 Hz, 1H), 7.30 – 7.21 (m, 5H), 6.91 (s, 1H), 6.35 (d, J = 8.0 Hz, 1H), 4.02 – 3.88 (m, 1H), 3.48 (s, 2H), 2.82 (d, J = 11.5 Hz, 2H), 2.15 (t, J = 10.6 Hz, 2H), 2.01 (d, J = 12.8 Hz, 2H), 1.59 (td, J = 12.4, 11.8, 5.9 Hz, 2H). ¹³C NMR (101 MHz, CDCl₃) δ 169.32, 164.55, 138.31, 133.67, 131.16, 129.15, 129.08, 128.72, 128.25, 127.08, 126.78, 126.43, 125.38, 124.50, 123.53, 63.02,

52.21, 47.08, 31.97. ESIMS m/z : 462.37 $[M + H]^+$ calcd for $C_{30}H_{27}N_3O_2 + H^+$ (461.57).

5-Benzylidene-3-(1-benzylpiperidin-4-yl)-2-(furan-2-yl)-3,5-dihydro-4H-

imidazol-4-one (AL04): Yield = 78 %, m.p. 217-219 °C. IR (KBr cm^{-1}) ν max: 3469, 3414, 3237, 2941, 1638, 1619, 1566, 1505, 1467, 1366, 1291, 1184, 758. 1H NMR (400 MHz, $CDCl_3$) δ 8.01 (s, 1H), 7.48 (d, J = 1.8 Hz, 1H), 7.46 – 7.39 (m, 2H), 7.34 (d, J = 13.2 Hz, 4H), 7.30 – 7.24 (m, 2H), 7.21 (d, J = 3.5 Hz, 1H), 7.00 (d, J = 3.0 Hz, 1H), 6.56 – 6.50 (m, 1H), 6.38 (d, J = 7.9 Hz, 1H), 4.01 – 3.82 (m, 2H), 2.88 (d, J = 11.4 Hz, 2H), 2.26 – 2.14 (m, 2H), 2.03 – 1.94 (m, 2H), 1.67 – 1.53 (m, 2H), 0.92 – 0.81 (m, 1H). ^{13}C NMR (101 MHz, $CDCl_3$) δ 164.81, 156.98, 146.92, 144.96, 137.24, 133.63, 129.38, 129.18, 128.94, 128.84, 128.34, 127.38, 126.97, 116.20, 112.57, 62.73, 52.02, 46.88, 31.54. ESIMS m/z : 430.35 $[M + H_2O]^+$ calcd for $C_{26}H_{25}N_3O_2 + H_2O^+$ (429.52).

5-Benzylidene-2-(furan-2-yl)-3-(2-(pyridin-4-yl)ethyl)-3,5-dihydro-4H-

imidazol-4-one (AL05): Yield = 72 %, m.p. 256-258 °C. IR (KBr cm^{-1}) ν max: 3478, 3415, 3238, 2032, 1638, 1617, 1467, 1354, 1298, 1185, 760. 1H NMR (400 MHz, $CDCl_3$) δ 8.50 (s, 1H), 8.28 (s, 2H), 7.37 (d, J = 3.4 Hz, 1H), 7.27 (s, 2H), 7.22 – 7.15 (m, 2H), 7.09 (d, J = 3.6 Hz, 1H), 6.99 (s, 2H), 6.77 (s, 1H), 6.40 (s, 1H), 3.38 (t, J = 6.6 Hz, 2H), 2.71 (t, J = 7.1 Hz, 2H). ^{13}C NMR (101 MHz, $CDCl_3$) δ 163.92, 155.23, 147.41, 146.22, 144.69, 142.95, 131.34, 127.14, 126.82, 126.57, 125.60, 122.19, 113.87, 110.27, 38.14, 32.54. ESIMS m/z : 362.21 $[M + H_2O]^+$ calcd for $C_{21}H_{17}N_3O_2 + H_2O^+$ (361.40).

5-Benzylidene-2-(furan-2-yl)-3-(2-(piperidin-1-yl)ethyl)-3,5-dihydro-4H-

imidazol-4-one (AL06): Yield = 75 %, m.p. 227-228 °C. IR (KBr cm^{-1}) ν max: 3434, 2933, 2853, 1638, 1619, 1509, 1470, 1352, 1296, 1183, 757. 1H NMR (400 MHz, $CDCl_3$) δ 8.09 (s, 1H), 7.45 (s, 1H), 7.39 (d, J = 6.5 Hz, 1H), 7.26 (dt, J = 12.0, 6.8 Hz, 3H), 7.16 – 7.08 (m, 2H), 6.46 (d, J = 5.5 Hz, 1H), 3.67 – 3.58 (m, 2H), 3.05 – 2.98 (m, 2H), 1.78 (d, J = 5.9 Hz, 4H), 1.53 – 1.48 (m, 3H), 1.20 (d, J = 10.8 Hz, 3H). ^{13}C NMR (101 MHz, $CDCl_3$) δ 165.98, 157.46, 147.03, 145.26, 133.59, 129.38, 129.04, 128.83, 128.31, 127.90, 115.96, 112.42, 57.23, 54.48, 34.98, 23.60, 22.65, 22.53. ESIMS m/z : 368.35 $[M + H_2O]^+$ calcd for $C_{21}H_{23}N_3O_2 + H_2O^+$ (367.14).

5-Benzylidene-3-(2-(1-benzylpiperidin-4-yl)ethyl)-2-(furan-2-yl)-3,5-dihydro-

4H-imidazol-4-one (AL07): Yield = 73 %, m.p. 205-207 °C. IR (KBr cm^{-1}) ν max: 3469, 3414, 3237, 2926, 1638, 1619, 1588, 1505, 1467, 1340, 1295, 1185, 759. 1H NMR (400 MHz, $CDCl_3$) δ 7.96 (s, 1H), 7.41 (dd, J = 1.8, 0.8 Hz, 1H), 7.37 – 7.30 (m, 2H), 7.28 – 7.19 (m, 8H), 7.12 (dd, J = 3.6, 0.8 Hz, 1H), 6.98 (s, 1H), 3.53 (s, 2H), 3.28 (dt, J = 7.9, 6.1 Hz, 2H), 2.93 – 2.84 (m, 2H), 2.03 (d, J = 10.3 Hz, 2H), 1.63 (d, J = 10.1 Hz, 2H), 1.48 – 1.38 (m, 2H), 1.26 – 1.12 (m, 3H). ^{13}C NMR (101 MHz, $CDCl_3$) δ 165.44, 165.41, 157.12, 146.93, 145.01, 133.63, 129.69, 129.23, 128.96, 128.80, 128.69, 128.36, 127.54, 116.14, 112.54, 62.85, 53.36, 37.73, 35.83, 33.08, 31.42. ESIMS m/z : 458.40 $[M + H_2O]^+$ calcd for $C_{28}H_{29}N_3O_2 + H_2O^+$ (457.57).

5-Benzylidene-2-(furan-2-yl)-3-(quinolin-8-yl)-3,5-dihydro-4H-imidazol-4-one

(AL08): Yield = 78 %, m.p. 261-263 °C. IR (KBr cm^{-1}) ν max: 3469, 3415, 3303, 3236, 1657, 1618, 1588, 1530, 1465, 1332, 1292, 756. 1H NMR (400 MHz, $CDCl_3$)

δ 10.56 (s, 1H), 8.77 (dd, $J = 7.2, 1.8$ Hz, 1H), 8.60 (dd, $J = 4.3, 1.6$ Hz, 1H), 8.11 – 8.03 (m, 2H), 7.52 – 7.41 (m, 4H), 7.38 – 7.24 (m, 4H), 7.22 – 7.16 (m, 1H), 6.51 (dd, $J = 3.5, 1.8$ Hz, 1H). ^{13}C NMR (101 MHz, CDCl_3) δ 163.08, 156.91, 148.25, 147.25, 144.88, 138.74, 136.26, 134.31, 133.80, 129.40, 129.15, 129.07, 128.89, 127.98, 127.93, 127.40, 121.85, 121.60, 116.79, 116.17, 112.57. ESIMS m/z : 384.10 $[\text{M} + \text{H}_2\text{O}]^+$ calcd for $\text{C}_{23}\text{H}_{15}\text{N}_3\text{O}_2 + \text{H}_2\text{O}^+$ (383.41).

5-Benzylidene-2-(furan-2-yl)-3-(quinolin-3-yl)-3,5-dihydro-4H-imidazol-4-one

(AL09): Yield = 77 %, m.p. 234-235 °C. IR (KBr cm^{-1}) ν max: 3661, 3444, 3064, 1447, 555, 508. ^1H NMR (400 MHz, MeOD) δ 8.79 (s, 1H), 8.72 (s, 1H), 7.86 (d, $J = 7.3$ Hz, 1H), 7.71 (s, 1H), 7.34 – 7.23 (m, 5H), 7.31-7.24 (m, 3H), 7.20 – 7.12 (m, 2H), 6.47 (s, 1H). ^{13}C NMR (101 MHz, DMSO) δ 165.38, 157.94, 147.64, 146.41, 145.82, 144.71, 134.45, 133.42, 130.09, 129.71, 129.48, 129.13, 128.97, 128.53, 128.21, 127.59, 123.74, 115.54, 112.60. ESIMS m/z : 384.10 $[\text{M} + \text{H}_2\text{O}]^+$ calcd for $\text{C}_{23}\text{H}_{15}\text{N}_3\text{O}_2 + \text{H}_2\text{O}^+$ (383.41).

3-([1,1'-Biphenyl]-2-yl)-5-benzylidene-2-(furan-2-yl)-3,5-dihydro-4H-imidazol-4-one (AL10):

Yield = 75 %, m.p. 209-210 °C. IR (KBr cm^{-1}) ν max: 3469, 3400, 3238, 1637, 1617, 1587, 1527, 1446, 1303, 1199, 1182, 750. ^1H NMR (400 MHz, CDCl_3) δ 8.57 – 8.46 (m, 1H), 8.07 (s, 1H), 7.54 – 7.49 (m, 1H), 7.42-7.39(m, 1H), 7.30 (s, 3H), 7.28 – 7.03 (m, 10H), 6.54 – 6.49 (m, 1H). ^{13}C NMR (101 MHz, CDCl_3) δ 162.39, 156.96, 146.70, 144.83, 137.86, 134.86, 133.42, 132.04, 130.08, 129.83, 129.29, 129.22, 128.88, 128.58, 128.08, 127.62, 124.17, 120.52, 116.36, 112.62. ESIMS m/z : 409.15 $[\text{M} + \text{H}_2\text{O}]^+$ calcd for $\text{C}_{26}\text{H}_{18}\text{N}_2\text{O}_2 + \text{H}_2\text{O}^+$ (408.46).

5-Benzylidene-2-(furan-2-yl)-3-(isoquinolin-3-yl)-3,5-dihydro-4H-imidazol-4-one (AL11):

Yield = 71 %, m.p. 249-251 °C. IR (KBr cm^{-1}) ν max: 3413, 3235, 1656, 1638, 1618, 1594, 1527, 1449, 1354, 1247, 1184, 758. ^1H NMR (400 MHz, CDCl_3) δ 8.90 (q, $J = 16.2, 13.2$ Hz, 2H), 8.71 – 8.60 (m, 1H), 8.02 (d, $J = 13.4$ Hz, 1H), 7.80 (q, $J = 13.1, 11.2$ Hz, 2H), 7.61 (s, 1H), 7.49-7.42 (m, 3H), 7.39 - 7.32(m, 3H), 7.26 – 7.18 (m, 1H) 6.57 – 6.45 (m, 1H). ^{13}C NMR (101 MHz, CDCl_3) δ 169.84, 163.42, 157.40, 151.05, 145.08, 130.78, 129.38, 129.01, 127.46, 126.98, 125.93, 116.62, 112.68, 108.63. ESIMS m/z : 384.35 $[\text{M} + \text{H}_2\text{O}]^+$ calcd for $\text{C}_{23}\text{H}_{15}\text{N}_3\text{O}_2 + \text{H}_2\text{O}^+$ (383.41).

5-Benzylidene-2-(furan-2-yl)-3-(5-methylthiazol-2-yl)-3,5-dihydro-4H-imidazol-4-one (AL12):

Yield = 74 %, m.p. 211-213 °C. IR (KBr cm^{-1}) ν max: 3438, 3416, 3220, 1651, 1605, 1571, 1526, 1439, 1307, 1182, 1178, 744. ^1H NMR (400 MHz, CDCl_3) δ 8.57 – 8.46 (m, 1H), 8.07 (s, 1H), 7.54 – 7.49 (m, 1H), 7.42-7.39 (m, 1H), 7.30 (m, 3H), 7.05 (s, 1H), 6.54 – 6.49 (m, 1H), 6.49 (d, $J = 13.4$ Hz, 1H), 2.09 (s, 3H). ^{13}C NMR (101 MHz, CDCl_3) δ 172.15, 168.19, 160.51, 141.09, 141.02, 138.57, 136.94, 134.13, 129.76, 129.05, 127.11, 119.38, 113.43, 112.27, 110.68, 29.53. ESIMS m/z : 354.79 $[\text{M} + \text{H}_2\text{O}]^+$ calcd for $\text{C}_{18}\text{H}_{13}\text{N}_3\text{O}_2\text{S} + \text{H}_2\text{O}^+$ (353.08).

Anti-inflammatory activity

The synthesized compounds were evaluated for anti-inflammatory activity. One-way analysis of variance (ANOVA) was performed to ascertain the significance of all the exhibited activities. The test compounds **AL01-AL12** and the standard drugs were administered in the form of a suspension (1% carboxymethylcellulose as a vehicle) by the oral route of administration. Each group consisted of six animals. The animals were maintained in colony cages at $25 \pm 2^\circ\text{C}$, relative humidity of 45–55%, under a 12 h light and dark cycle; were fed standard animal feed.²²All the animals were acclimatized for a week before use.

Anti-inflammatory activity was evaluated by a carrageenan-induced paw edema test in rats.²³ Diclofenac sodium 10 and 20 mg/kg was administered as standard drug for comparison. The test compounds were administered at two dose levels of 10 and 20 mg/kg. The paw volumes were measured using the mercury displacement technique with the help of a plethysmograph immediately before and 30 min, 1, 2, and 3 h after carrageenan injection. The percent inhibition of paw edema was calculated according to the following formula, percent inhibition $I = 100[1 - (a - x)/(b - y)]$ where x is the mean paw volume of rats before the administration of carrageenan and test compounds or reference compound (test group), a is the mean paw volume of rats after the administration of carrageenan in the test group (drug-treated), b is the mean paw volume of rats after the administration of carrageenan in the control group, y is the mean paw volume of rats before the administration of carrageenan in the control group. All the percent inhibition results are shown in Table 2.

Anticancer activity (MTT Assay)

To evaluate the initial screening of 12 compounds, MTT Colorimetric assay was performed on HCT116 (Human colorectal cancer cell line) and HeLa (Human cervical cancer cell line). Cells were checked for 80% confluency. The culture media was removed and cells were gently washed with media which was followed by the addition of trypsin solution to it. The plate with trypsin was incubated in a CO_2 incubator at 37°C for 3–4 min. It was then observed under a bright-field microscope for the detachment of the cells. To inhibit the action of trypsin, media was added to it in the ratio of 1:2. This mixture was centrifuged at 2000 rpm for 5 min. The cell pellet was resuspended in the appropriate amount of complete media and further processed for cell count with Trypan blue dye using a hemocytometer. The cells were seeded in triplicates in a 96-well cell culture plate for both the cell lines at a seeding density of 7×10^3 per well and incubated at 37°C in a humidified CO_2 incubator for 24 h for cell growth. The next day, treatment of compounds to the respective wells at a concentration of $10\mu\text{M}$ was given and the individual plates were incubated at 37°C in a humidified CO_2 incubator for both 48 h and 72 h respectively. After individual incubation hours, MTT reagent of working concentration 0.5 mg/ mL was added to each well and the plate wrapped in a foil paper was incubated at 37°C in a humidified CO_2 incubator for 4 h. Post incubation, media was removed carefully and 50 μL of DMSO was added to dissolve formazan crystals and incubated for 15–20 min. Absorbance was measured at 570 nm.

Results and Discussion

In-silico Predictions of Molecular Properties and ADMET

Pharmacokinetic studies of test derivatives **AL01-AL12** were estimated using the online Swiss ADME tool and Osiris property explorer, in which molinspiration (physicochemical properties) and toxicity were predicted and presented (Table 1 and 2). The results depicted that all the synthesized analogs satisfied and obey the Lipinski five rule.

Table 1
Molecular properties of synthesized compounds (AL01-AL12) by molinspiration

Compound code	MW (g/mol)	Log P ^a	TPSA ^b	OH-NH interact ^c	O-N interact ^d	nrotb ^e
AL01	320.44	1.52	22.08	0	4	2
AL02	270.38	0.32	22.08	0	4	2
AL03	397.48	3.89	49.05	0	5	4
AL04	411.50	3.81	49.05	0	5	5
AL05	426.52	3.24	61.94	0	6	6
AL06	432.57	3.22	52.29	0	6	6
AL07	522.69	4.94	52.29	0	6	8
AL08	365.39	3.70	58.70	0	5	3
AL09	365.39	3.58	58.70	0	5	3
AL10	390.44	5.04	45.81	0	4	4
AL11	365.39	3.93	58.70	0	5	3
AL12	335.39	3.44	86.94	0	5	3

^a Calculated octanol/water partition coefficient; ^b Molecular polar surface area; ^c Number of hydrogen-bond donors; ^d Number of hydrogen-bond acceptors; ^e Number of rotatable bonds.

Table 2
Calculation of Osiris toxicity risk of synthesized compounds (AL01-AL12)

Compound code	Drug-likeness / Drug-score	Osiris Toxicity Risk Calculation			
		M	T	I	R
AL01	6.40/0.56	-	-	-	-
AL02	5.74/0.96	-	-	-	-
AL03	7.20/0.47	-	-	-	-
AL04	7.59/0.46	-	-	-	-
AL05	6.06/0.47	-	-	-	-
AL06	5.82/0.47	-	-	-	-
AL07	8.75/0.33	-	-	-	-
AL08	1.94/0.46	-	-	-	-
AL09	1.80/0.28	-	-	-	-
AL10	0.75/0.34	-	-	-	-
AL11	1.80/0.45	-	-	-	-
AL12	2.74/0.50	-	-	-	-

[M] Mutagenicity; [T] Tumorigenicity; [I] Irritating effects; [R] Reproductive effects; [-] No risk fragment indicating related effects.

A computational study for the prediction of drug-likeness and toxicity properties of all molecules was performed and presented in Table 3. All the tested compounds showed moderate prediction results of drug-likeness calculation depending on the molinspiration web tool. The positive results without great risk of toxicity have recorded support in Osiris.

The selection of prime potential drug molecules was consolidated as a therapeutic agent. However, those may fail in clinical trials and exist adverse effects. Hence, in the drug discovery process to predict the reach of synthesized compounds into the target site the essential parameter used is pharmacokinetic parameters. From Table 3 observed the ADME properties of synthesized derivatives by their significant results.

Table 3
ADME properties of the synthesized compounds (AL01-AL12)

Compound code	BBB ^a	PgP ^b	HIA ^c	BS ^d	SA ^e
AL01	Yes	No	High	0.55	3.9
AL02	No	No	High	0.55	3.69
AL03	Yes	No	High	0.55	4.77
AL04	Yes	No	High	0.55	3.56
AL05	Yes	No	High	0.55	3.87
AL06	Yes	Yes	High	0.55	4.75
AL07	Yes	Yes	High	0.55	3.64
AL08	Yes	No	High	0.55	3.65
AL09	Yes	No	High	0.55	3.83
AL10	Yes	No	High	0.55	3.67
AL11	No	No	High	0.55	3.6
AL12	Yes	No	High	0.55	3.9

^aBlood-Brain Barrier penetration, ^b P-glycoprotein substrate, ^c Human Intestinal Absorption,

^d Bioavailability, ^e Synthetic accessibility

In the drug discovery process, the physicochemical properties, pharmacokinetics, and toxicity studies of tested drugs are essential for qualifying in clinical trials. On this aspect, the molecular properties of the synthesized derivatives were predicted in molinspiration online tools. Based on the Lipinski rule, molecular weight, hydrogen donor/acceptor, and non-rotational bonds of the synthesized motifs produced their affordable result towards their molecular properties. Additionally, the polar surface area was also showed significant value, which is accountable for their oral bioavailability. Transport characteristics of molecules like blood-brain barrier penetration and intestinal absorption were determined from molecular volume. Based on the existing literature, these afforded values were referred to. Based on the results of the Lipinski rule and ADMET the synthesized motifs were optimized for further studies. In any case, the presence of a good drug score in this part of the molecule was very effective for the activity.

Molecular Docking Study

From the targeted molecular simulations, it was found that the title analogs produced significant results in all tested targets and the obtained results are presented in Table 4. The docking score for synthesized derivatives (**AL01-AL12**) on COX-1 (PDB ID: 3KK6) produced a significant result in the range of **-5.11 to -8.35** Kcal/mole compared with diclofenac -8.12 Kcal/mole noted in table 4. Among the thirteen compounds, **AL01** were afforded highly significant results as **-8.35** Kcal/mole and produced its potency through binding affinity towards the targeted enzyme by hydrophilic and hydrophobic interactions were shown in Figure 1A & 1B.

Table 4
Docking score of synthesized compounds (AL01-AL12) on COX-1

Ligands	Docking score (kcal/mole) COX-1 (3KK6)	Binding site Amino acid residues	
		Hydrogen bond Interactions	Hydrophobic bond Interactions
AL01	-8.35	His A:386	His A:207, 388; Trp A:387; Ala A:202; Leu A:390.
AL02	-6.46	His B:207	His B:386, 388; Phe B:210
AL03	-6.53	Gln A:370	Glu A:543; Asn A:122
AL04	-5.91	His A:386	His A:207; Phe A:210; Thr A:212; Val A:291, 447; Ile A:444;
AL05	-6.17	His B:388	Ala A:202; His B:207, 446; Ile B:444; Val B:447; Leu B:408;
AL06	-6.73	His A:207; Gln A:203	Ala A:202; Leu A:390, 294, 295; His A: 388; Ile A: 444; Met A:391
AL07	-5.11	His B: 386	His B: 207, 388; Val B:447
AL08	-6.41	-	Pro A:84; Leu A:92, 93, 112, 115; Trp A: 100; Ile A:89; Val A:116, 119.
AL09	-6.61	-	Leu B:123; Arg B:83, 120; Glu B:524; Ile B: 89; Leu B: 112; Val B:119.
AL10	-7.19	His B:207; Thr B:212	Lys B:211; Val B:291
AL11	-6.69	-	Pro B:162; Arg B:157, 456, 459; Leu B:171
AL12	-7.56	Arg B:374; Arg A:374	Val B:145; Pro B:538.
DICLOFENAC	-8.12	Phe B:142; Gly B:536	Phe B:210; Asn A:376, 426; His B:226

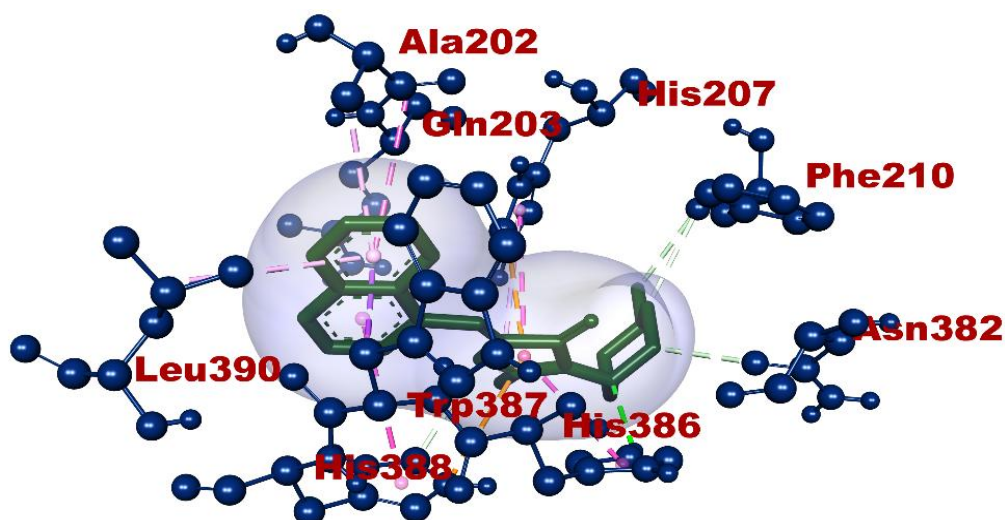
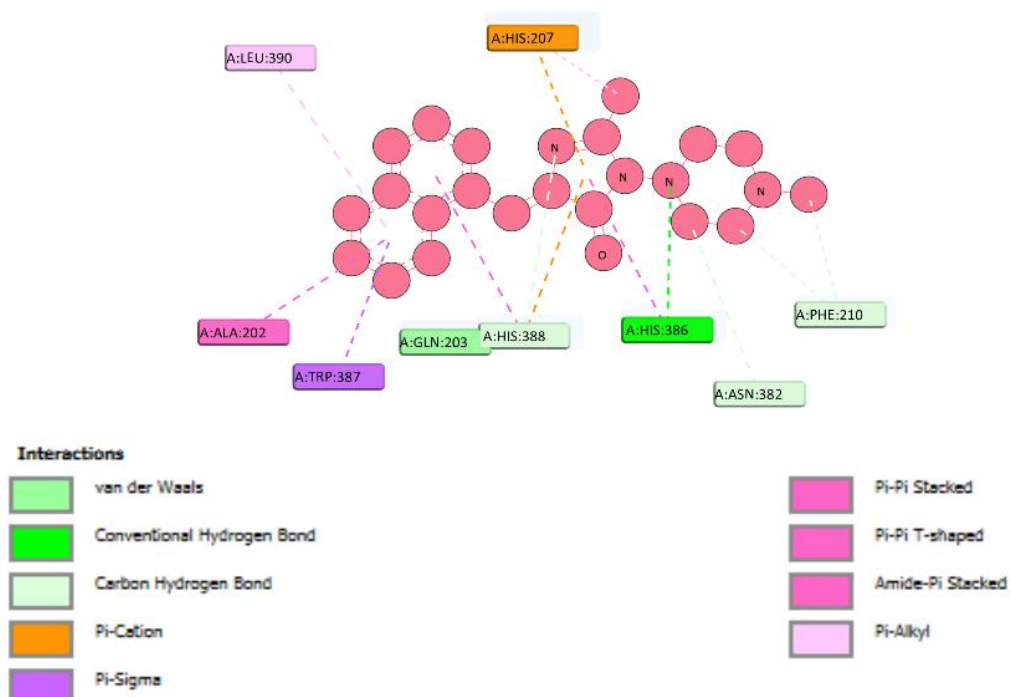


Figure 1A. Molecular interactions between AL01 and COX-1 by Biovia discovery studio visualizer.
(A) Docked pose of AL01 and COX-1 binding site.



(B) Hydrogen bond interactions on AL01 and COX-1 (green dashed lines) and Hydrophobic bonds (Pink dashed lines) and other amino acid residues

The second target of molecular docking study is **COX-2** (Cyclooxygenase-2), in which all tested derivatives were found to be noteworthy binding affinity towards this receptor. Among which, **AL11** showed high binding scores such as -8.39kcal/mole respectively) compared with diclofenac -8.93 Kcal/mole were mentioned in Table 5 and the binding pose of **AL11** represented in Figure 2A & 2B.

Table 5
Docking score of synthesized compounds (AL01-AL12) on COX-2

Ligands	Docking score (kcal/mole) COX-2 (3LN1)	Binding site Amino acid residues	
		Hydrogen bond Interactions	Hydrophobic bond Interactions
AL01	-7.96	Gly A:30; Asn A:19, 24; Gln A:447.	Ala A:142; Cys A:21,32; Pro A:139; Tyr A:116.
AL02	-7.90	Gln C:447; Asn C:24; Arg C:29, 455; Lys C:454; Glu C:451.	Leu C:138; Lys C:454
AL03	-5.52	Asn A:19; His C:193	Ala B:142; Pro A:139; Leu D:138;
AL04	-6.27	Ser B:107, 112	Pro A:528.
AL05	-8.15	Lys A:454; Gln A:27	Leu A:138; Pro A:139; Arg A:29; Cys A:21, 32.
AL06	-6.26	Gly D:121; Gln C:313	Cys D:21; Asp D:143; Tyr D:122; His D: 119
AL07	-5.31	Thr C:198; His C:193	Lys C:197; His C:372.
AL08	-8.03	Asn C:28	Lys C:454; Arg C:455, 29; Leu C:458; Ser C:457.
AL09	-7.95	Gln B:313	Tyr A:122; Cys A:21, 32; Pro A:139; Ala A:142.
AL10	-7.35	Asp B:143; Gln A:313	Pro B:139, 140; Ala B:142, Tyr B:122
AL11	-8.39	Tyr A:116	Glu A:31; Cys A:32; Leu A:138; Pro A: 139; Cys A:21
AL12	-7.42	Arg D:29	Cys D:21; Lys D:454; Glu D:451; Arg D:455; Leu D:138; Pro D:139; Cys D:32.
DICLOFENAC	-8.93	Arg C:29; Asn D:19;	Lys D:454; Gln D:27; Glu C:451

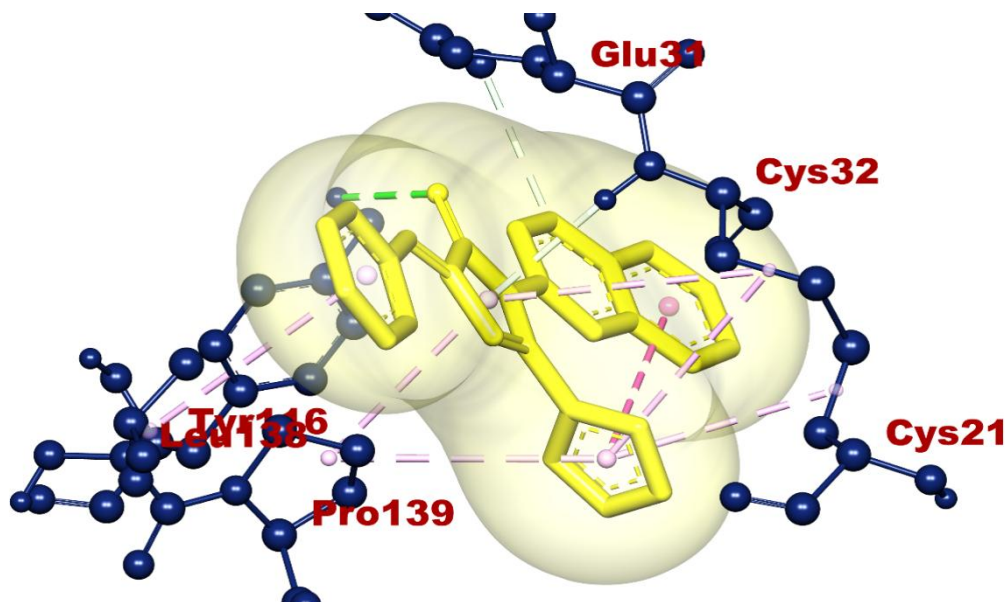
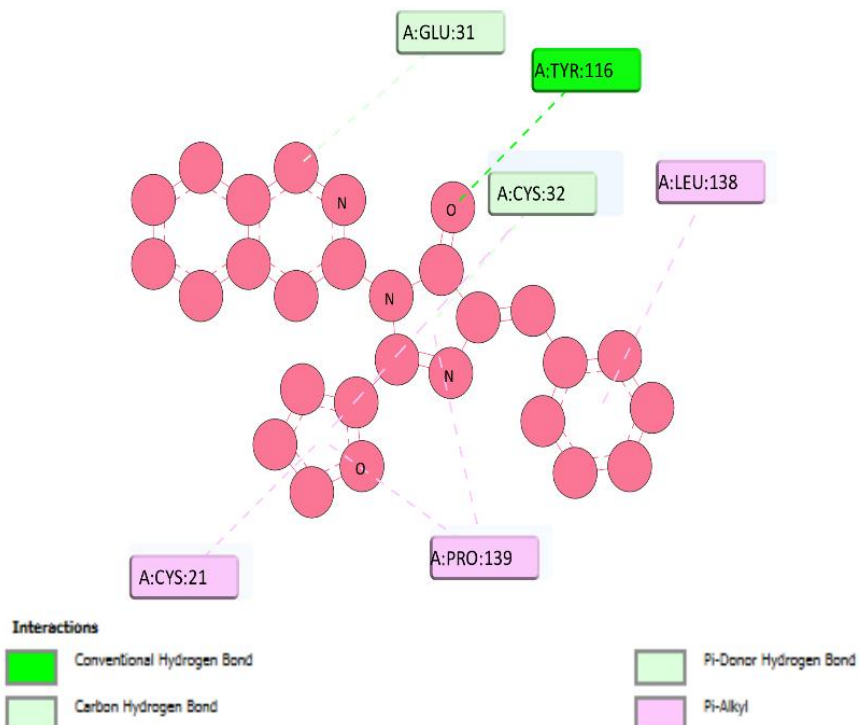


Figure 2. Molecular interactions between AL11 and COX-2 by Biovia discovery studio visualizer.

(A) Docked pose of AL11 and COX-2 binding site.



(B) Hydrogen bond interactions on AL11 and COX-2 (green dashed lines) and Hydrophobic bonds (Pink dashed lines) and other amino acid residues.

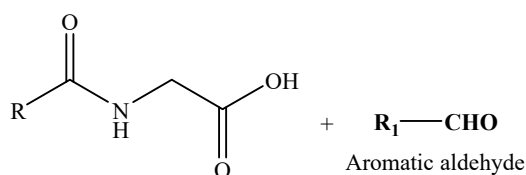
The cyclooxygenase (COX-1 and COX-2) are important isozymes that catalyze the complex biotransformation of arachidonic acid into PGs and thromboxanes, which are ultimately responsible for many physiological and pathophysiological responses. The COX-1 isozyme facilitates homeostatic functions including cytoprotection of the gastric mucosa, the start of labor pain, regulation of renal blood flow, and platelet aggregation. Recently, experimental results have identified a likely involvement of COX-1 in angiogenesis, therefore providing the basis for the development of COX-1 inhibitors. On the other hand, the COX-2 isozyme is principally responsible for the production of inflammatory PGs that induce pain, swelling, and fever. Apart from its ability to induce peripheral inflammation, the expression of COX-2 isozyme is up-regulated in several human cancers such as gastric, breast, lung, colon, esophageal, prostate, and hepatocellular carcinomas.

Chemistry

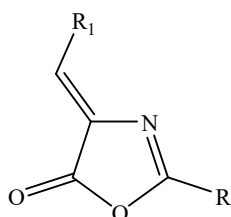
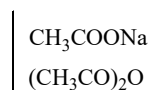
CHEMISTRY

Various novel imidazolones (**AL01-AL12**) were synthesized from N-substituted glycine and aromatic aldehyde by a multistep synthesis as per the protocol shown in Scheme. Initially, N-substituted glycine and aromatic aldehyde undergoes Erlenmeyer-Plöchl azlactone synthesis and produced 2,4-disubstituted oxazol-5(4*H*)-one (**III-VI**) in presence of sodium acetate and acetic anhydride. In the next step, the obtained 2,4-disubstituted oxazol-5(4*H*)-one (**III-VI**) undergoes substitution reaction with various aromatic/heterocyclic amines in presence of acetic acid and produces novel 1,2,4-trisubstituted-1*H*-imidazol-5(4*H*)-ones (**AL01-AL12**). To optimize the reactions for purity and completion, TLC was performed throughout the reactions.

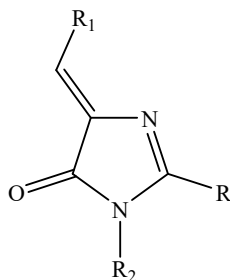
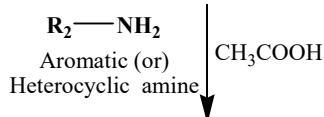
Assigned structures of the test compound were confirmed using various spectral studies (IR, NMR, and mass spectral analysis). The presence of particular groups was identified from IR spectra using some characteristic absorption peaks. The disappearance of a sharp peak around 3300 cm^{-1} in IR corresponds to N-H stretching indicates the formation of 2,4-disubstituted oxazol-5(4*H*)-one (**III-VI**). The formations of compound **III-VI** were confirmed by the appearance of singlet around $\delta\ 7.00$ ppm for single protons in its $^1\text{H-NMR}$ spectra which might be assigned to =CH group. The appearance of the characteristic peak corresponds to aromatic C-H, aliphatic C-H, carbonyl group, C=N, C=C in IR spectrum in the specified range indicates the formation of novel imidazolones (**AL01-AL12**). In addition, the appearance of various peaks in the NMR spectrum corresponding to attached aromatic/heterocyclic amine confirms the formation of novel imidazolones (**AL01-AL12**). Mass spectrum further confirmed their molecular weight and purity.



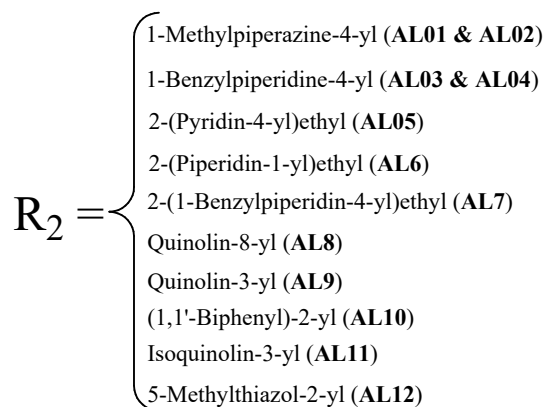
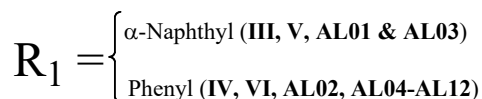
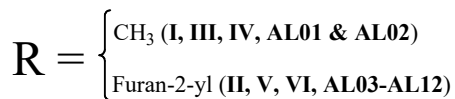
N-Substituted glycine (**I-II**)



2,4-Disubstituted
oxazol-5(4*H*)-one (**III-VI**)



1,2,4-Trisubstituted-1*H*-
imidazol-5(4*H*)-one (**AL01-AL12**)



Scheme: Synthesis of novel imidazolones (AL01-AL12)

Anti-inflammatory activity

Carrageenan induced paw edema test was employed in *Wistar* rats to estimate the anti-inflammatory potency of imidazole-5(4*H*)-one derivative **AL01-AL12** and the obtained results are summarized in Table 6. Entire title compounds displayed significant activity with a graded dose-response. The anti-inflammatory activity of novel imidazole-5(4*H*)-ones **AL01-AL12** were varied with reaction time. Generally, imidazole-5(4*H*)-one analog showed moderate anti-inflammatory activity at 30 minutes of reaction time and the activity increased at 1st hour. Further,

anti-inflammatory activity reached to peak level at the 2nd hour, and decreased activity was seen at the 3rd hour.

Among twelve tested compounds, **AL01 & AL02** were found to be a more potent anti-inflammatory derivative that exhibits more activity than reference diclofenac. These two compounds possess methyl substituent at the C-2 position of imidazole-5(4*H*)-one ring which may be responsible for the potent activity. The rest of all derivatives **AL03 - AL12** possess furan ring at the C-2 position. Compounds **AL11 & AL12** displayed very good anti-inflammatory activity which is equipotent to standard diclofenac. These compounds **AL11 & AL12** possess isoquinoline and 5-methyl thiazole ring, respectively at the N-1 position of imidazole-5(4*H*)-one ring. Title derivatives **AL08, AL09 & AL12** displayed moderate anti-inflammatory activity compared to diclofenac. These moderate active anti-inflammatory agents **AL08, AL09 & AL12** possess 2-(1-benzylpiperidin-4-yl)ethyl, quinoline-8-yl, and quinoline-3-yl substituent, respectively at the N-1 position of imidazole-5(4*H*)-one ring. The rest of the tested compounds **AL03 - AL07** exhibited weaker anti-inflammatory activity. From the study the most potent anti-inflammatory agents were found to be 2-methyl-1-(4-methylpiperazin-1-yl)-4-(naphthalen-1-ylmethylene)-1*H*-imidazol-5(4*H*)-one **AL01**, and 4-benzylidene-2-methyl-1-(4-methylpiperazin-1-yl)-1*H*-imidazol-5(4*H*)-one **AL02**. Among twelve tested title compounds, 4-benzylidene-1-(2-(1-benzylpiperidin-4-yl)ethyl)-2-(furan-2-yl)-1*H*-imidazol-5(4*H*)-one **4** exhibited worst anti-inflammatory activity.

Table 6
Percent anti-inflammatory activity of the synthesized compounds AL01-AL12

Compound code	Dose (mg/kg)	Percent protection			
		30 min	1 h	2 h	3 h
AL01	10	34±0.75**	42±1.19*	50±1.03*	37±0.92***
	20	47±1.47*	60±1.21*	74±1.08**	50±0.55*
AL02	10	32±1.62*	40±0.65*	47±1.31*	36±0.67*
	20	45±0.59*	59±1.42***	71±1.35**	49±1.04*
AL03	10	12±2.13*	18±1.60*	22±1.04*	14±1.56 ^{NS}
	20	18±1.56*	22±2.37 ^{NS}	31±1.92**	18±0.48*
AL04	10	10±0.91 ^{NS}	15±1.94**	19±0.87*	10±2.16*
	20	14±1.18*	19±1.73*	26±2.50 ^{NS}	17±1.02**
AL05	10	14±1.14 ^{NS}	19±0.98*	22±1.66**	15±0.71*
	20	18±0.59***	25±1.84*	33±0.21 ^{NS}	21±2.09*
AL06	10	12±2.35*	16±1.58 ^{NS}	21±1.39*	11±0.87**
	20	16±0.90*	22±1.53**	27±1.20*	18±0.65 ^{NS}
AL07	10	09±0.50*	13±1.35 ^{NS}	16±2.19*	10±0.82*
	20	11±1.78 ^{NS}	18±0.41*	24±0.96**	13±2.14*
AL08	10	21±2.01*	27±1.04*	30±1.85*	20±0.79***
	20	27±0.97*	44±2.13*	48±0.82*	28±1.21*
AL09	10	23±0.96**	31±1.09*	33±0.40*	23±2.23*
	20	30±1.23*	47±0.62*	53±0.94*	32±1.57**
AL10	10	21±1.45*	28±1.05**	33±2.17*	22±0.64 ^{NS}
	20	29±0.36*	45±0.61*	50±1.50*	31±0.91*
AL11	10	30±0.52**	40±1.27*	46±0.78*	32±2.35**

	20	43±0.44*	56±1.36*	70±0.51***	44±1.78*
AL12	10	28±1.17*	39±0.70**	44±2.15 ^{NS}	32±0.69*
	20	42±0.79**	54±0.58*	67±1.63*	43±1.30**
Control	NA	04±0.37	06±0.83	04±0.56	04±0.49
Diclofenac	10	30±1.06**	39±1.71*	45±1.19*	33±0.84***
	20	42±0.89*	57±1.65**	68±1.02*	45±0.70**

Each value represents the mean ± SEM (n=6);^{NS}: Non-significant; Significance levels: *p < 0.5, **p < 0.01, ***p < 0.001 as compared with the respective control.

Anticancer activity (MTT Assay)

Initial screening of various compounds on different cell lines such as HCT116, HeLa, MDA-MB-231, and MCF-7 was performed by MTT colorimetric assay for 48 and 72 h. Out of the screened results we got of different compounds, only 1 compound (**AL-10** at 72 h in HCT116 cancer cell line) showed less than 50% viability.

Conclusion

In summary, a set of novel imidazol-5(4*H*)-one analog were designed, synthesized, and characterized using various analytical techniques like FT-IR, ¹H-NMR, Mass spectroscopy, and elemental analysis. Molinspiration online tool was used to predict the molecular properties and molecular docking was used to predict the anti-inflammatory potency of title analogs. All synthesized imidazol-5(4*H*)-ones were screened for their *in-vivo* anti-inflammatory activity by carrageenan-induced rat paw edema test. Diclofenac was used as a reference standard for comparison. Test compounds displayed poor to excellent (9 to 74 %inflammation protection) anti-inflammatory activity. Generally, from the study it was found that compounds having methyl substituent (**AL01 & AL02**) at the C-2 position of imidazole-5(4*H*)-one ring displayed superior activity than compounds possessing furan ring (**AL03-AL12**) at the C-2 position. Within methyl substituent analogs(**AL01 & AL02**), compounds having naphthalen-1-ylmethylene (**AL01**) at the C-4 position of imidazole-5(4*H*)-one ring displayed better activity than compounds possessing benzylidene (**AL02**) at the C-4 position. In addition, *in vitro* anticancer potency of test compounds was estimated by the MTT assay method and found that most of the tested analogs were found to be inactive at tested concentration against the tested cell lines. From the study the most potent anti-inflammatory agents were found to be 2-methyl-1-(4-methylpiperazin-1-yl)-4-(naphthalen-1-ylmethylene)-1*H*-imidazol-5(4*H*)-one **AL01**, and 4-benzylidene-2-methyl-1-(4-methylpiperazin-1-yl)-1*H*-imidazol-5(4*H*)-one **AL02**. Hence, these analogs might be extended as a novel class of anti-inflammatory agents with additional structural variations to improve the anti-inflammatory potencies.

Acknowledgments

The authors are thankful to Vels Institute of Science, Technology & Advanced Studies (VISTAS), for the facilities extended.

Conflicts of interest

The authors declare that they have no conflicts of interest.

References

1. S.V. Bhandari, S.C. Dangre, K.G. Bothara, A.A. Patil, A.P. Sarkate and D.K. Lokwani, *Eur. J. Med. Chem.*,44, 4622 (2009).
2. G. Dannhardt and W. Kiefer, *Eur. J. Med. Chem.*,36, 109 (2001).
3. S. Saravanan, P.S. Selvan, N. Gopal, J.K. Gupta, and B. De, *Archiv der Pharmazie: An International Journal Pharmaceutical and Medicinal Chemistry*, 338(10), 488 (2005).
4. A. Siwach, P.K. Verma, *BMC Chemistry*, 15, 12 (2021).
5. L.H. Al-Wahaibi, B.G. Youssif, E.S. Taher, A.H. Abdelazeem, A.A. Abdelhamid, and A.A. Marzouk, *Molecules*, 26(16), 4718 (2021).
6. C. Bamoro, F. Bamba, K.T.D. Steve-Evanes, V. Aurélie, and C. Vincent, *Open Journal of Medicinal Chemistry*, 11(2), 17 (2021).
7. C.M. Gallati, S.K. Goetzfried, M. Ausserer, J. Sagasser, M. Plangger, K. Wurst, M. Hermann, D. Baecker, B. Kircher, and R. Gust, *Dalton Transactions*, 49(17), 5471 (2020).
8. A. Valls, J.J. Andreu, E. Falomir, S.V. Luis, E. Atrián-Blasco, S.G. Mitchell, and B. Altava, *Pharmaceuticals*, 13(12), 482 (2020).
9. S.S. Alghamdi, R.S. Suliman, K. Almutairi, K. Kahtani, and D. Aljatli, *Drug Design, Development, and Therapy*, 15, 3289 (2021).
10. J.G. Lombardino, and E.H. Wiseman, *Journal of Medicinal Chemistry*, 17(11), 1182 (1974).
11. A.K. Gopalakrishnan, S.A. Angamaly, and M.P. Velayudhan, *ChemistrySelect*, 6(40), 10918 (2021).
12. M. Bian, Q.Q. Ma, Y. Wu, H.H. Du, and G. Guo-Hua, *Journal of Enzyme Inhibition and Medicinal Chemistry*, 36(1), 2139 (2021).
13. A. Verma, S. Joshi, and D. Singh, *Journal of Chemistry*, (2013).
14. X.L. Ma, C. Chen, and J. Yang, *Acta Pharm Sin*, 26(4), 500 (2005).
15. R. Mannhold, . Molecular drug properties-Measurement and prediction. Wiley-VHC Verlag GmbH & Co. KGaA: Weinheim, Germany, 30, (2008).
16. Y.H. Zhao, J. Le, M.H. Abraham, A. Hersey, P.J. Eddershaw, C.N. Luscombe, D. Boutina, G. Beck, B. Sherborne, I. Cooper, and J.A. Platts, *J. Pharm. Sci.*,90(6), 749(2001).
17. C. Björkelid, T. Bergfors, A.K.V. Raichurkar, K. Mukherjee, K. Malolanarasimhan, B. Bandodkar, and T.A. Jones, *J. Biol. Chem.*, 288(25), 18260 (2013).
18. S.M. Batt, T. Jabeen, V. Bhowruth, L. Quill, P.A. Lund, L. Eggeling, L.J. Alderwick, K. Fütterer, and G.S. Besra, *Proceedings of the National Academy of Sciences*,109(28), 11354 (2012).
19. A. Wehenkel, P. Fernandez, M. Bellinzoni, V. Catherinot, N. Barilone, G. Labesse, M. Jackson, and P.M. Alzari, *FEBS letters*, 580(13), 3018 (2006).
20. S.R. Luckner, C.A. Machutta, P.J. Tonge, and C. Kisker, *Structure*, 17(7), 1004 (2009).
21. X.Y. Meng, H.X. Zhang, M. Mezei, and M. Cui, *Curr. Comput. Aided Drug Des.*, 7(2), 146 (2011).
22. E.D. Olfert, B.M. Cross, and A.A. McWilliam, Canadian council of animal care guide to the care and use of experimental animals, Vol 1, 2nd edn (1993).
23. C.A. Winter, E.A. Risley, and G.W. Nuss, *Exp. Biol. Med.*,111, 544 (1962).